



Levels, spatial distribution, risk assessment, and sources of environmental contamination vectored by road dust in Cienfuegos (Cuba) revealed by chemical and C and N stable isotope compositions

Yasser Morera-Gómez¹ · Carlos Manuel Alonso-Hernández¹ · Jesús Miguel Santamaría² · David Elustondo² · Esther Lasheras² · David Widory³

Received: 25 April 2019 / Accepted: 15 October 2019 / Published online: 26 November 2019
© Springer-Verlag GmbH Germany, part of Springer Nature 2019

Abstract

Road dust is an indicator widely used when monitoring contamination and evaluating environmental and health risks in urban ecosystems. We conducted an exhaustive characterization of road dust samples coupling their chemical characteristics and stable isotope compositions (C and N) with the aim of evaluating the levels and spatial distribution of local contamination as well as to identify its main source(s) in the coastal city of Cienfuegos (Cuba). Results indicate that the concentrations of several elements (total nitrogen, S, Ca, V, Cu, Zn, Mo, Sn, Hg, and Pb) exceed the background values reported for both Cuban soils and the upper continental crust (UCC) and showed a high variability among the sampling sites. We show that road dust contamination in Cienfuegos induces high associated ecological risks. Among the studied elements, Cd and Hg are the major contributors to the environmental contamination in the city, mainly along busy roads and downtown. $\delta^{13}\text{C}$ and $\delta^{15}\text{N}$, coupled to a multivariate statistical analysis, help associate the studied elements to several local sources of contamination: mineral matter derived from local soils, cement plant and related activities, road pavement alteration, power plant, road traffic, and resuspension of particulate organic matter (POM). Our results suggest that incorporating the chemical and isotope monitoring of road dust may help implement more effective environmental management measures in order to reduce their adverse impact on ecosystems and human health.

Keywords Road dust · Chemical composition · $\delta^{13}\text{C}$ and $\delta^{15}\text{N}$ · Contamination assessment · Multivariate analysis · Cuba

Introduction

Pollution is one of the major issues affecting our environment today (WHO 2016). In particular, pollution in urban areas has

reached epic proportions, essentially as a result of rapid industrialization and urbanization, becoming an environmental concern worldwide (Modabberi et al. 2018). The level and chemical composition of dust particles deposited on roads and streets are among the indicators most used to study the health of urban ecosystems (Christoforidis and Stamatis 2009; Li et al. 2013, 2019; Lanzerstorfer 2018; Skrbic et al. 2018; Bourliva et al. 2018).

Road dust is a unique indicator of urban pollution because (i) it is ubiquitous on roads and highways, (ii) it is of both natural and anthropogenic origins, and (iii) it reflects recent deposition as well as the alteration of old materials (LeGalley et al. 2013). Most of the road dust is composed of (i) naturally occurring geogenic elements (e.g., Al, Ti, Fe...), (ii) elements from the roadside soil, and (iii) elements resulting from the alteration of the pavement (Shi and Lu 2018; Keshavarzi et al. 2018). In addition, resuspension of deposited particles deriving from road traffic usually represents the main anthropogenic component of road dust in urban areas worldwide (Soltani et al. 2015; Men

Responsible editor: Philippe Garrigues

Electronic supplementary material The online version of this article (<https://doi.org/10.1007/s11356-019-06783-7>) contains supplementary material, which is available to authorized users.

✉ Yasser Morera-Gómez
yasser@ceac.cu

¹ Centro de Estudios Ambientales de Cienfuegos (CEAC), AP 5. Ciudad Nuclear, 59350 Cienfuegos, CP, Cuba

² Laboratorio Integrado de Calidad Ambiental (LICA), Universidad de Navarra, C/Irunlarrea s/n, 31008 Navarra, Spain

³ Geotop/Université du Québec à Montréal (UQAM), 201 Ave Président Kennedy, Montreal, QC, Canada

et al. 2018; Zhang et al. 2019). This is why road dust is usually scrutinized to determine the chemical profile of road traffic emissions (Sternbeck et al. 2002).

Road traffic is one of the major sources of airborne particles in urban environments, and the fine particles it is generating have been proved to have deleterious health and environmental effects (Ferreira-Baptista and De Miguel 2005; e.g. Bourliva et al. 2017). Air contamination related to road traffic affects the population living close to busy roads as well as at larger spatial scales since emissions can be transported over long distances (Pateraki et al. 2019). Road dust is also a reservoir of harmful substances, in particular potentially toxic elements emitted by industries, hospitals, solid waste deposits, wastewaters, construction activities, painting, pavement alteration, among other urban sources. This may also endanger other connected environments, such as water bodies subject to contamination resulting from stormwater and wastewater discharges (LeGalley et al. 2013; Modabberi et al. 2018). These discharges, often under the form of road runoff, contain traditional contaminants, such as micro pollutants, organic matter, heavy metals, polycyclic aromatic hydrocarbons (PAH), and perfluorinated compounds, but also emergent contaminants such as microplastics and microrubbers, which can cause a significant alteration of the receiving waters quality (Sutherland and Tolosa 2000; Kojima et al. 2017; Abbasi et al. 2017; Škrbić et al. 2019; Ghanavati et al. 2019).

As a consequence, governments as well as national and international organizations have designed and implemented policies dedicated to reducing the impact of this contamination and, in general, of human activities in urban environments, especially in coastal areas (Manuel Trujillo-Gonzalez et al. 2016; Lloyd et al. 2019). But measuring the actual impact of these policies on the environmental quality of ecosystems is difficult. Unfortunately, the availability of contamination data time series in urban coastal areas is very limited and very dispersed geographically.

The city of Cienfuegos, located on the Caribbean coast of southern Cuba, has not been exempt from pollution issues (Fattorini et al. 2004). For decades, local authorities have dedicated resources and efforts to monitor air and water quality in its coastal zones (Seisdedo et al. 2016; Morera-Gómez et al. 2018a; Seisdedo et al. 2019). Thus, characterizing the levels and characteristics (e.g., temporal, spatial distributions, and types) of emissions from potential sources that may contaminate air and receiving waters in urban and coastal zones is a critical step to establish efficient environmental mitigation strategies and/or to evaluate the results of the already implemented policies.

With that in mind, we conducted an exhaustive chemical characterization coupled to a study of the stable C and N isotope compositions of several road dust samples from the coastal mid-size city of Cienfuegos in Cuba. Our main objectives were to assess the levels, spatial distribution, and

ecological risks and to identify the main source(s) of local contamination. To this end, we applied different approaches, including index of pollution, stable isotope fractionation, and multivariate analysis (PCA and cluster analysis). Ultimately, we discussed the implication for human health and the environment.

Methods

Study area

Cienfuegos city, with a population of ~ 160,000 inhabitants, is an important tourist and industrial center in Cuba, located in the south center part of the country on the coast of the Caribbean Sea (Fig. 1). A significant number of potential air contamination sources are present within and around this urbanized area, including a large petroleum refinery, a thermal power plant, a cement plant, a harbor, large pier areas and ship breaking yards, coal storage and packing, scrap storage and classification sites, very intense transportation activities including ferrous scrap trucks and busy ports used for transportation, and heavy road traffic that mostly runs on diesel (Fig. 1). Several villages and agricultural areas and some resorts are also located in the region (Fig. 1). The region is typical of the Caribbean Sea climate, characterized by two distinct dry (approximately from May to October) and wet (November to April) seasons. During the last three decades, the average annual rainfall has been 1363 mm, mostly during the wet period (~ 80%). The yearly prevalent wind direction in the area is ENE. Meteorological data were provided by the meteorological center of the Cienfuegos city.

Road dust sampling

A total of 31 road dust samples were collected from the main paved roads of Cienfuegos city (Fig. 1) by sweeping an area of about 1.0 m × 0.5 m from pavement edges using a plastic dustpan and brushes. Samples were mainly collected at road intersections. The sampling was conducted on July 20, 2016 (wet season), under sunny and windless conditions and with no rain having occurred (i.e., having washed the pavement) during the three days prior to sampling. All samples were stored and labeled in self-sealed polyethylene bags and immediately brought back to the laboratory for preparation and analysis. In the laboratory, samples were dried at 45 °C, passed through a 50-μm sieve and stored in polyethylene bags until further analysis.

Chemical analysis

Concentrations of 49 major and trace elements (Be, Na, Mg, Al, P, S, K, Ca, V, Ti, Cr, Mn, Fe, Co, Ni, Cu, Zn, As, Rb, Sr,

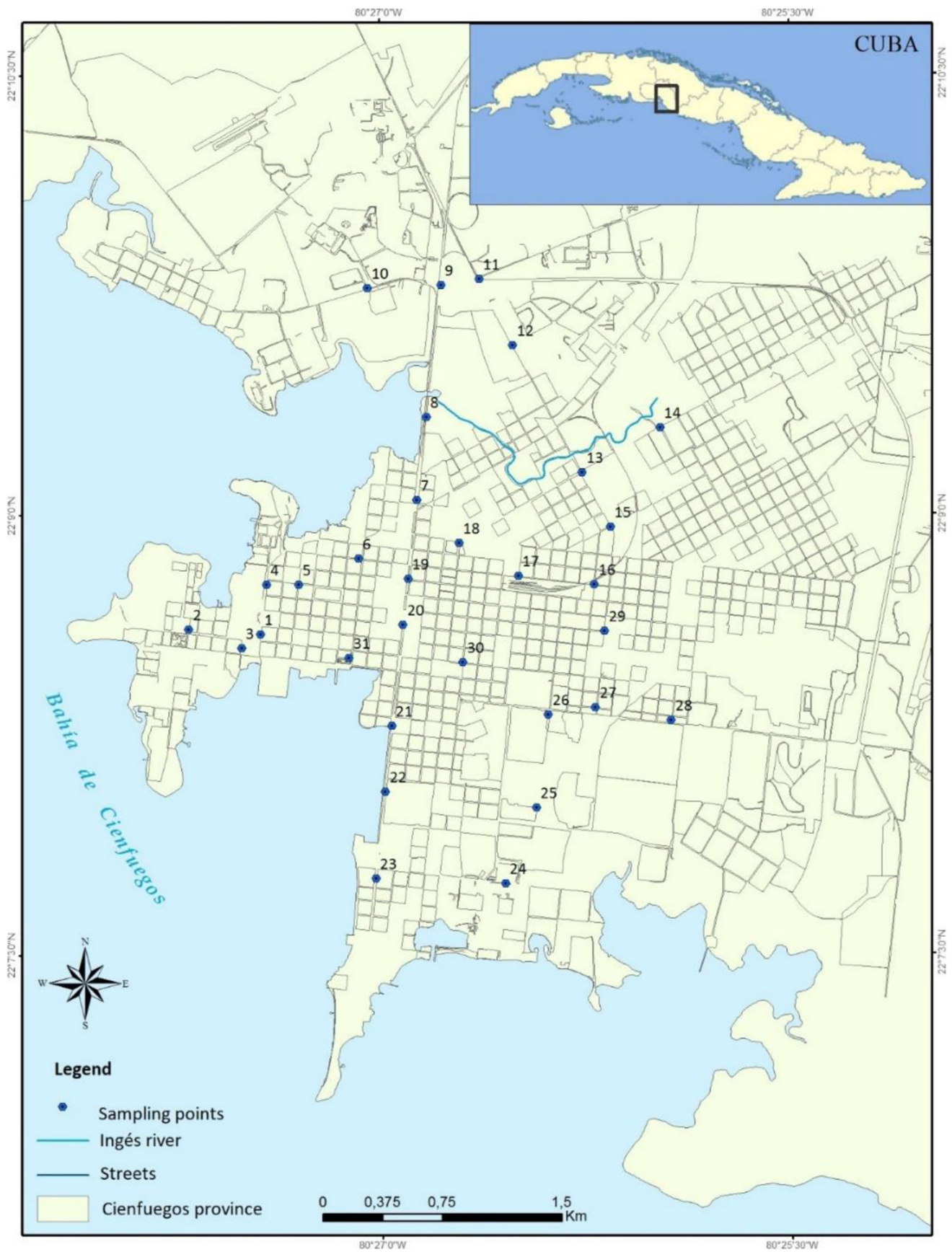


Fig. 1 Study area showing sampling point locations

Cd, Sn, Sb, Cs, Ba, La, Ce, Pr, Nd, Sm, Eu, Gd, Dy, Ho, Er, Tm, Yb, Lu, Hf, Tl, Pb, Th, U, Ge, Zr, Nb, Mo, W, Hg) were conducted on the road dust samples using inductively coupled plasma mass spectrometry (ICP-MS, Agilent 7500a). The methodology used was the same than the one described in Morera-Gómez et al. (2018a). An aliquot (50 mg) of each road dust sample was digested with HF, H₂O₂, HNO₃, and HCl (3:3:4:1 mL) in a closed microwave digestion system (CEM Co., Mars X press). A multi-element solution (Li, Sc, Y, In, Bi) was added to the sample and indium (In) was used as the internal standard for further determination by ICP-MS. Mercury (Hg) concentrations were determined by atomic absorption spectrometry (AAS) using a Mercury Analyzer (MA-2000 Series, Nippon) on a second 50-mg road dust sample.

Quality assurance of the analytical results was controlled by repeated analysis of the certified reference materials (CRMs) CTA-FFA1 and 0217-CM-73007 for major and trace elements and Hg, respectively. Elemental recoveries, the relative standard deviation (RSD) obtained from the CRMs, and the method detection limits (DLs) are provided in Table S1 (Online Resource 1). In addition, several samples were analyzed in duplicate. The number of replicates and the average RSD are also provided in Table S1 (Online Resource 1).

Total carbon, total nitrogen, and stable C and N isotope composition analysis

Concentrations of the total carbon (TC) and total nitrogen (TN) and their corresponding stable isotope compositions ($\delta^{13}\text{C}$ and $\delta^{15}\text{N}$) were determined using an elemental analyzer (Vario MICRO Cube, Elementar, Hanau, Germany) coupled to an isotope ratio mass spectrometer (IsoPrime 100, Cheadle, UK) operating in continuous flow mode. Inorganic carbon (carbonate) was not removed prior to the isotope analysis. For the analysis, about 4 mg of road dust was packed into a tin capsule and introduced into the EA autosampler. Isotope compositions are expressed as $\delta^{13}\text{C}$ and $\delta^{15}\text{N}$ values, which represent the relative difference expressed in per mil (‰) between the isotope ratio of the sample and that of a standard (Pee Dee Belemnite (PDB) for carbon and atmospheric N₂ for nitrogen):

$$\delta^{13}\text{C} (\text{‰vs.PDB}) = \left[\left(R_{\text{sample}} / R_{\text{standard}} - 1 \right) \right] \times 1000 \quad (1)$$

$$\delta^{15}\text{N} (\text{‰vs.AIR}) = \left[\left(R_{\text{sample}} / R_{\text{standard}} - 1 \right) \right] \times 1000 \quad (2)$$

where $R = {}^{13}\text{C}/{}^{12}\text{C}$ or ${}^{15}\text{N}/{}^{14}\text{N}$.

The analytical quality control was performed by routine analysis of interspersed international carbon and nitrogen isotope standards (IAEA, Vienna, Austria) and the interlaboratory-calibrated algae reference material 1452 B (University of Barcelona). We also ran several samples in duplicate. The obtained reproducibility was < 0.2‰ for C and < 0.3‰ for N

stable isotope compositions. Similarly, analytical uncertainties for TC and TN concentrations were within 2 and 3% of the reported values, respectively.

Calculations for assessing contamination levels

Different geochemical methods were used to quantify the degree of contamination in the road dust samples:

Enrichment factors

Enrichment factors (EFs) were calculated in order to determine a possible anthropogenic contribution to the measured major and trace element concentrations. EF were calculated as follows:

$$EF_X = (C_X / C_R)_{\text{road dust}} / (C_X / C_R)_{\text{UCC}} \quad (3)$$

where X represents the element of interest; EF_X the EF of X ; C_X the concentration of X ; and C_R the concentration of a reference element. In this study, titanium (Ti) was selected as the reference element. The upper continental crust (UCC) chemical composition was used for normalization (Rudnick and Gao 2014). According to their EF values, elements can be classified into three contamination categories (Dehghani et al. 2017): $EF < 2$ is considered a deficiency to a minimal enrichment, $2 < EF < 10$ represents a moderate enrichment and $EF \geq 10$ a high enrichment.

Pollution load index

The pollution load index (PLI), for a given sampling site, was calculated using the following formula (Tomlinson et al. 1980):

$$PLI = \sqrt[n]{C_f^1 \times C_f^2 \times C_f^3 \times \dots \times C_f^n} \quad (4)$$

$$C_f^i = \frac{C_{\text{sample}}^i}{C_{\text{UCC}}^i} \quad (5)$$

where C_f^i is the pollution factor of the element i (of a total of n elements) and C_{sample}^i and C_{UCC}^i are the sample and background concentrations of element i , respectively. A PLI value > 1 indicates a polluted road dust, whereas $PLI < 1$ indicates no pollution (Tomlinson et al. 1980).

Similarly, the pollution load index for a zone (PLI_{zone}) was calculated by considering the PLI of each sampling site in the following equation:

$$PLI_{\text{zone}} = \sqrt[m]{PLI_1 \times PLI_2 \times PLI_3 \times \dots \times PLI_m} \quad (6)$$

where m is the number of sampling sites considered (31 in our case).

Potential ecological risk index

The potential ecological risk index (RI), originally introduced by Hakanson (1980), was also calculated to estimate the degree of contamination of road dust by toxic heavy metals using the following equation:

$$RI = \sum E_r^i = \sum T_r^i \times C_f^i = \sum T_r^i \times \frac{C_{\text{sample}}^i}{C_{\text{UCC}}^i} \quad (7)$$

where RI stands for the ecological risk of multiple elements and E_r^i is the potential ecological risk of each element i . T_r^i is the metal toxic factor. The following T_r^i values were considered: Mn = Zn = Sr = Ti = 1, V = Cr = 2, Cu = Co = Ni = Pb = 5, As = Sb = 10, Cd = 30, and Hg = 40 (Hakanson 1980; Li et al. 2018b). Five categories are used to describe the different risk levels according to their E_r^i value: $E_r^i < 40$ represents a low risk; $40 < E_r^i < 80$ a moderate risk; $80 < E_r^i < 160$ a considerable risk; $160 < E_r^i < 320$ a high risk; and $E_r^i > 320$ a very high risk. On the other hand, RI values are categorized into four categories: $RI < 150$ low risk, $150 \leq RI < 300$ moderate risk, $300 \leq RI < 600$ considerable risk, and $RI \geq 600$ very high risk (Hakanson 1980).

Statistical analysis and mapping

Statistical analysis, including Spearman correlation, cluster analysis, and principal component analysis (PCA) were conducted using the SPSS v.15 software package (IBM Corporation, Armonk, NY). The maps reporting the pollution indexes spatial distribution were generated using Kriging as the interpolation method for the 31 road dust samples (3DFieldPro v.4.3.1.0 software (<http://3dfmaps.com/>)).

PCA with VARIMAX rotation and Kaiser normalization were used to identify the possible sources of the variance for the different elements that were measured. Prior to the statistical analysis, the data set distribution was evaluated using the Lilliefors normality test. When the distribution was not normal, data were transformed using the Box-Cox transformation from the package *AID* included in the software R (Asar et al. 2017). Several elements that yielded $EF < 2$ were removed from the PCA in order to decrease the number of variables. After that, the Kaiser-Meyer-Olkin (KMO) value of the sampling adequacy (> 0.5) and the significance level of the Barlett's test of sphericity (< 0.001) indicated that the data was suitable for the multivariate statistical analysis. Finally, principal components were extracted from the variables with eigenvalues > 1 , and the PCA results were only accepted when (i) the sum of those principal components accounted for more than 75% of the total variance of the dataset, and (ii) all the communality values were ≥ 0.6 . A hierarchical cluster analysis (HCA) using the Ward's method and the Euclidean

distance was also performed to identify similarly contaminated sites.

Results and discussion

Chemical composition of road dust

The mean concentrations, range of variations (minimum and maximum values), and standard deviations for each element analyzed are reported in Table S2 (Online Resource 1). The UCC values (Rudnick and Gao 2014) and background values for Cuban soils (Alfaro et al. 2015, 2018) are also reported for comparison purpose in Table S2. Results indicate that the concentrations for TN, S, Ca, V, Cu, Zn, Mo, Sn, Hg, and Pb in our road dust samples are higher than the corresponding background values for both Cuban soils and the UCC. Cr, Ni, As, Cd, and Sb concentrations were higher than the UCC values but similar or slightly lower than the background values for Cuban soils. In addition, the concentrations for TN, P, S, Cu, Zn, As, Mo, Sn, Sb, W, Hg, and Pb varied greatly among the different sampling sites ($RSD > 40\%$), which may suggest contributions from numerous distinct anthropogenic sources (Abbasi et al. 2017; Keshavarzi et al. 2018; Xu et al. 2018). The average Hg concentrations, equivalent to 9.8 and 4.9 times the UCC and the Cuban soil background values, respectively, showed the highest heterogeneity with a RSD of 127%.

When compared to those of other urban areas in the world (reported in Table S3 in the Online Resource 1), levels of Cr, Cu, Zn, and Pb were higher in Cienfuegos than those observed in Camagüey (Díaz Rizo et al. 2015), a bigger Cuban city, while Fe, Co, and Ni were similar. In general, the mean Ca, Rb, and V concentrations in the present study were significantly higher than those reported in other urban environments worldwide. Several potential sources for these elements are present within the study area, such as the cement plant located 25-km ENE (under the prevalent wind direction) of Cienfuegos that is fueled by petroleum-coke as well as the power plant located within the city (near sampling site no. 10) that is fueled by Cuban heavy crude oil. The highest Ca concentrations may also correspond to emissions from construction and repair activities largely operating in the city during recent years. Other potential sources include asphalt pavement weathering and shipping emissions. Morera-Gómez et al. (2018a, 2019) recently measured high Ca and V concentrations in PM_{10} and atmospheric bulk deposition samples in Cienfuegos that the authors attributed to these sources. Similarly, average concentrations for Cu, Mo, Hg, and Pb were comparable to those reported in other more industrialized and developed cities, such as Ottawa, Luanda, or Beijing (Rasmussen et al. 2001; Ferreira-Baptista and De Miguel 2005; Yu et al. 2016). These elements are commonly

associated with both exhaust and non-exhaust road traffic emissions (Johansson et al. 2009; Grigoratos and Martini 2015; Adamiec et al. 2016). Road traffic in Cuba is mainly dominated by very old cars running on diesel, a feature that is recognized for enhancing the levels of heavy metals originating from the fuel, the lubricating oil motor, brake, and tire wear (Das et al. 2017). All other elements are within the range of variations reported for the cities listed in Table S3 (Online Resource 1), which usually are bigger, more industrialized, and developed than Cienfuegos.

The Spearman correlation analysis showed that elements with a typical crustal origin such as Na, K, Al, Fe, Mn, Ge, Ti, Zr, and the lanthanoid elements (La to Lu) were strongly and positively correlated (with r values usually > 0.6 ; $p < 0.01$) confirming a common origin. While Ca was also strongly correlated with these elements, its correlation coefficient was negative indicating it has a distinct origin. Cu was found to be uncorrelated with most of the studied elements but showed strong correlations with Pb ($r = 0.8$, $p < 0.01$), Fe ($r = 0.7$, $p < 0.01$), Sn ($r = 0.7$, $p < 0.01$), and Sb ($r = 0.8$, $p < 0.01$), indicating that these elements originate from a single source, probably related to road traffic emissions since these element are their typical tracers (Johansson et al. 2009; Grigoratos and Martini 2015). Similarly, V–Ni ($r = 0.7$, $p < 0.01$), Cr–Co ($r = 0.6$, $p < 0.01$), Cr–Ni ($r = 0.7$, $p < 0.01$), Cu–Hg ($r = 0.6$, $p < 0.01$), Zn–Ni ($r = 0.6$, $p < 0.01$), Zn–Hg ($r = 0.7$, $p < 0.01$), S–Mo ($r = 0.6$, $p < 0.01$), As–Sb ($r = 0.6$, $p < 0.01$), Sb–Hg ($r = 0.5$, $p < 0.01$), and Pb–Hg ($r = 0.5$, $p < 0.01$) were found to be significantly correlated, maybe suggesting the influence of emissions from other anthropogenic sources. The significant correlations observed between Hg and several heavy metals also suggest distinct sources for this pollutant, in agreement with its high variability in the studied urban area. In addition, V and As were significantly correlated ($r > 0.5$, $p < 0.01$) with most of the crustal elements aforementioned, hinting that they may also have a crustal origin.

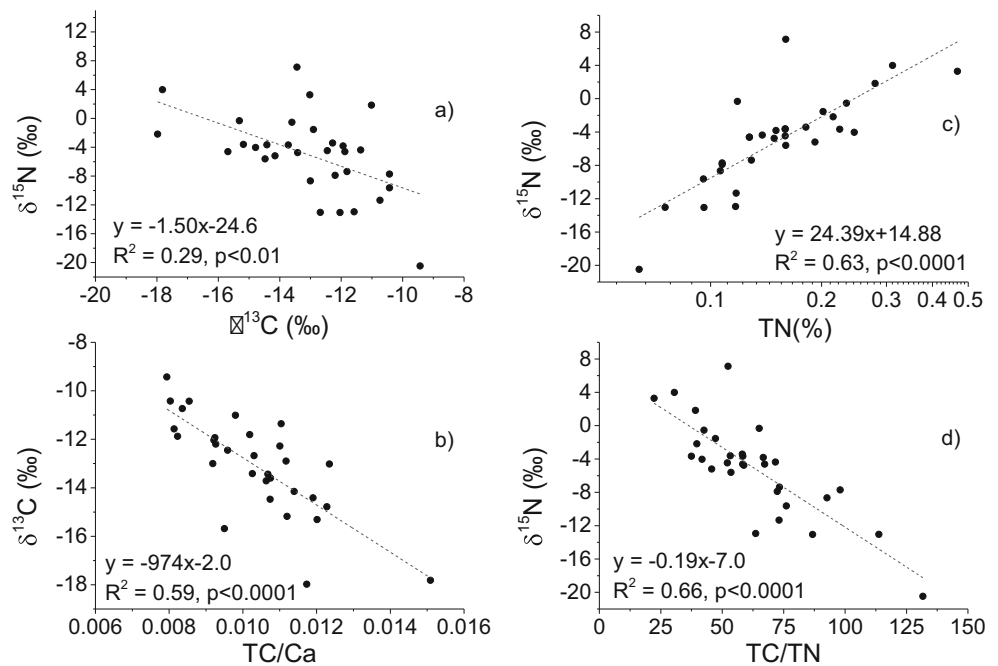
These results evidence that elements such as V have both natural and anthropogenic origins. While the average V/Ni ratio (2.9 ± 0.6) lied within the range of natural geological materials (2–3), several sampling sites yielded ratios in the range of 3–4, typical of oil combustion (Moreno et al. 2010). On the other hand, La/V ratios (0.07 ± 0.02) exhibited very low values compared to those of mineral particulate matter coming from uncontaminated crustal materials or coal combustion (typical values around 0.2–0.3; Moreno et al. 2008; Celo et al. 2012), indicating a strong influence of emissions from oil and/or petroleum-coke combustion. Similar results were recently reported in PM₁₀ and atmospheric bulk deposition collected in Cienfuegos (Morera-Gómez et al. 2018a, 2019). Other indicators, such as the La/Ce ratio (average of 0.45 ± 0.02 ; within the range of crustal materials (0.4–0.6); Moreno et al. 2010), confirmed the crustal origin of the lanthanoid elements in the study area.

Stable carbon and nitrogen isotope compositions

The stable C and N isotope compositions of road dust samples collected in Cienfuegos are shown in Fig. 2a. Both $\delta^{13}\text{C}$ and $\delta^{15}\text{N}$ displayed large variations from -18.0 to -9.4‰ (average of $-13.1 \pm 2.0\text{‰}$) and from -20.5 to 7.1‰ (average of $-5.0 \pm 5.6\text{‰}$), respectively. $\delta^{13}\text{C}$ and $\delta^{15}\text{N}$ were roughly correlated ($r = -0.54$, $p < 0.01$), suggesting that both C and N contents may be controlled by common sources and processes. A recent study by Morera-Gómez et al. (2018b) characterized the $\delta^{13}\text{C}$ of aerosols emitted by several sources of contamination in Cienfuegos: soot particles from the combustion of diesel ($\delta^{13}\text{C} = -26.3\text{‰}$) and gasoline ($\delta^{13}\text{C} = -25.2\text{‰}$), shipping ($\delta^{13}\text{C} = -25.7\text{‰}$), and power plant ($\delta^{13}\text{C} = -27.1 \pm 0.2\text{‰}$) as well as local soils ($\delta^{13}\text{C} = -20.5 \pm 4.8\text{‰}$). While our road dust samples were all enriched in ^{13}C relative to these sources, they showed $\delta^{13}\text{C}$ similar to the one measured in a bulk deposition sample collected in the vicinity of the cement plant (-15.3‰). Their $\delta^{13}\text{C}$ were similar to those measured in cement ($-11.6 \pm 2.0\text{‰}$) and kiln ($-15.5 \pm 0.5\text{‰}$) dust samples in a cement plant in Barcelona (Mari et al. 2016). These results suggest that the cement plant and its related activities (construction, work in quarries, transportation of cement and raw materials...) are controlling the $\delta^{13}\text{C}$ signature of road dust in Cienfuegos. As previous studies mostly report more ^{13}C -depleted isotope compositions (Lopez-Veneroni 2009; Kawashima and Haneishi 2012; e.g. Bandowe et al. 2018) compared to our road dust samples, it also comes that, unlike Cienfuegos, other cities worldwide usually are not affected by emissions from cement plant activities. Supporting the above hypothesis, the $\delta^{13}\text{C}$ showed a good correlation with the C/Ca ratio ($r = -0.77$, $p < 0.01$; Fig. 2b), which is consistent with a ^{13}C -enrichment resulting from the presence of carbonates that have typical $\delta^{13}\text{C}$ centered around 0‰ (Kump and Arthur 1999). $\delta^{13}\text{C}$ values also strongly correlated with the Ca concentrations ($r = 0.76$, $p < 0.01$) but not with the TC concentrations, which probably reveals several contributing sources.

On the other hand, the large range of $\delta^{15}\text{N}$ (from -20.5 to 7.1‰) measured in our road dust samples overlapped those reported by Morera-Gómez et al. (2018b) for soot particles from the combustion of diesel ($\delta^{15}\text{N} = 1.7\text{‰}$) and gasoline ($\delta^{15}\text{N} = -1.8\text{‰}$), shipping ($\delta^{15}\text{N} = 3.0\text{‰}$), soil samples ($\delta^{15}\text{N} = 1.0 \pm 2.8\text{‰}$), and a bulk deposition sample collected from the vicinity of the cement plant ($\delta^{15}\text{N} = 5.6\text{‰}$) in Cienfuegos. In contrast, our $\delta^{15}\text{N}$ were depleted in ^{15}N with respect to the power plant emissions ($\delta^{15}\text{N} = 11.4 \pm 3.4\text{‰}$). This suggests that several distinct sources are contributing to the overall TN budget in road dust and/or that secondary processes ultimately modify the initial $\delta^{15}\text{N}$ (i.e., these secondary processes induce nitrogen isotope fractionations). The fact that $\delta^{15}\text{N}$ showed a ^{15}N enrichment with the increasing TN content (Fig. 2c) supports the hypothesis that secondary processes are controlling

Fig. 2 a–d Variations of C ($\delta^{13}\text{C}$) and N ($\delta^{15}\text{N}$) stable isotope compositions of road dust samples collected in Cienfuegos with TN and C/Ca and C/N ratios



the final N content in road dust. This ^{15}N enrichment was also observed with the decreasing TC/TN ratio (Fig. 2d).

If the trends we are observing between $\delta^{15}\text{N}$ -TN and $\delta^{15}\text{N}$ -TC/TN (Fig. 2c, d) actually reflect the formation of secondary nitrogen, it can be assumed that the road dust particles having the lowest TN are mostly representative of the source(s) of primary nitrogen (e.g., their TN is mostly controlled by primary nitrogen as they are lowly affected by secondary processes and thus contain low secondary nitrogen). Taking also into account that all particles we analyzed from the emission sources in Cienfuegos present TN and TC/TN ratios similar or higher to the highest values observed in our road dust samples (Morera-Gómez et al. 2018b), we can assume that (1) secondary processes result in a ^{15}N depletion (i.e., $\delta^{15}\text{N}$ decrease with decreasing TN) and, as particles from local top soils (TN = $0.6 \pm 0.3\%$ and TC/TN = 20.4 ± 10.2) yielded $\delta^{15}\text{N}$ consistent with the isotope ranges, we measured for high-TN in road dust, that (2) top soils represent a potential source of primary nitrogen. Degraded terrestrial particulate organic matter (POM) have typical values of TC/TN (Andrews et al. 1998) that are consistent with the ratios we measured in road dust that had the highest $\delta^{15}\text{N}$. In addition, García-Moya (personal communication, 2019) showed that POM in wastewater from Cienfuegos is characterized by $\delta^{15}\text{N} = 0.7 \pm 2.4\%$, TN = $3.6 \pm 1.4\%$, and TC/TN = 7.8 ± 0.6 , and thus may also be considered a source of primary nitrogen. Other potential sources include animal wastes, with typical $\delta^{15}\text{N}$ between 0 and 25‰ (Kojima et al. 2011; Alonso-Hernández et al. 2017), since horse-drawn carriages are commonly used for transportation in Cienfuegos and can generate a substantial amount of organic matter on roads.

Ultimately, the processes that explain the positive relationship observed in Fig. 2c (or negative in Fig. 2d) may be two-fold: (1) the production of nitrates by nitrification that induces a ^{15}N depletion (e.g., Amiri et al. 2015), followed by (2) a dilution by runoff during the frequent wet season rainfalls in Cuba that will result in a decrease in the TN content (Kojima et al. 2011) without affecting the corresponding $\delta^{15}\text{N}$. In order to confirm that hypothesis further studies focusing on samples collected during the dry period and the determination of their corresponding $\delta^{15}\text{N}$ - NO_3^- are needed.

Assessment and spatial distribution of contamination

EF from major and trace elements showed that TN, Cd, Hg, and Pb were highly enriched (Fig. 3), indicating they are mainly emitted by anthropogenic sources. Ca, S, Sb, Sn, Mo, Zn, and Cu were, in average, moderately enriched ($2 \leq \text{EF} \leq 10$) but several sampling sites yielded high EF > 10 that suggest these are also significantly impacted by anthropogenic sources. P, V, Cr, and Rb presented EF around 2, suggesting relatively low anthropogenic contributions. The rest of the elements were predominantly of natural origin with EF < 2. It can be noted that among the most enriched elements (EF > 4.9 in Fig. 3), sampling sites 03, 06, 09, 14, 18, and 19 gave even higher EF that reached 100 for total nitrogen at site 14. These sites are all located along or near busy roads. This confirms that emissions related to road traffic (e.g., exhaust or brake tire and pavement wear...) is a major source for these elements (Cu, Zn, Pb, Cd, Sb, Sn, Hg, Mo, and S), in agreement with recent studies (e.g., Abbasi et al. 2017; Alves et al. 2018; Keshavarzi et al. 2018). The high N enrichment

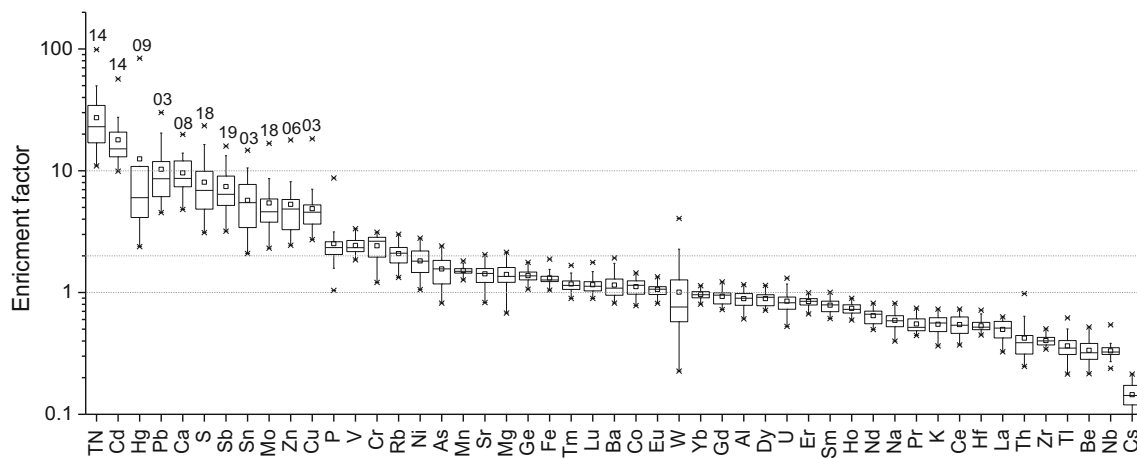


Fig. 3 Elemental enrichment factors (EF) in road dust samples from Cienfuegos, Cuba. Numbers refer to sample sites reported in Fig. 1

observed in some of the road dust samples may result from the input of soil particles that in Cienfuegos present N contents significantly higher than the UCC values (Morera-Gómez et al. 2018b), but also from the input of organic matter. As previously discussed, horse-drawn carriage is a very common mean of transportation in Cienfuegos and sampling site 14 (where the total nitrogen EF of 100 was measured; Fig. 3) is located on one of its most common routes. Another possible source of organic matter is wastewater overflows that usually occur in many roads and sites throughout the city (Soonthornnonda and Christensen 2008).

Fifty-eight percent of the PLI calculated in Cienfuegos was higher than 1, with variations from 0.77 to 1.43 and an average value of 1.07 ± 0.15 . The distribution pattern for PLI_s is shown in Fig. 4a. PLI tended to increase towards downtown (sampling sites 1–6 and 31), the city main avenue (sampling sites 7, 19–21), near the train station (sampling site 16, near the intersection of the railway with the road), the urban residential area (sampling site 29), and one of the main highways entering the city (sampling sites 11–12). Road traffic is more concentrated in those areas. Additionally, the PLI_{zone} calculated for Cienfuegos was 1.06. That corresponds to a slightly polluted urban area on the classification scale.

To better understand the pollution degree of 14 potentially toxic heavy metals, we also calculated their corresponding potential ecological risk indexes E_r^i (Table 1). E_r^i values for V, Cr, Mn, Co, Ni, Zn, As, Sr, and Ti were all < 40 . These elements present thus a low ecological risk. The mean E_r^i value for Cu was < 40 although site 03, located near busy roads and a motor garage, showed a higher index ($E_r^i = 67$), indicative of a moderate ecological risk. Pb and Sb with average indexes of 40 and 57, respectively, presented a moderate ecological risk, whereas Cd (average E_r^i of 398) and Hg (average E_r^i of 392) showed a very high risk. Furthermore, the calculated RI was > 300 for all sites and even > 600 for 19 of the 31 sites, which indicates a considerable to very high ecological risk in the study area. Both, Cd and Hg, contributing to

42% of the total RI, appear as priority pollutants to be included in the monitoring of road dust in Cienfuegos. The spatial distributions of RI (Fig. 4b) was similar to that of PLI (Fig. 4a) and identified 6 well-defined hotspots: 4 located downtown and along busy roads (sites 1, 6, 7–19, 21, and 14), 1 near the train station (site 16), and a last one on one of the city highways (site 9, with the highest RI value, mainly controlled by its high Hg E_r^i). These results demonstrate that road dust in Cienfuegos is contaminated by heavy metals that have high associated ecological risks. These conclusions confirm that contamination of road dust in Cienfuegos should be a concern for local authorities as these elements threaten both ecological and human health (Wei et al. 2009; e.g. Li et al. 2018b).

Source identification and site classification

The PCA results allowed to define 5 principal components accounting for 77% of the total variance. We used the factor loadings higher than 0.5 (highlighted in italics in Table 2) to identify the most probable sources of contamination. Factor 1 (F1), explaining 35.1% of the total variance, was characterized by high positive K, Na, Mn, Fe, Ti, and As factor loadings coupled to negative Ca and TC ones. This indicates that the mineral fraction of the soil contributes to the urban road dust, as most of these positively correlated elements are both typically of crustal origin and presented minimal enrichments. Moreover, the significant negative Ca and TC factor loadings indicate $CaCO_3$ inputs from sources such as cement production and transportation, construction, and other activities that can generate contamination by direct emissions, resuspension, and atmospheric deposition. The significant As factor loading (0.702) confirms its crustal origin as well as, to a lesser extent, for V (0.390). Factor 2 (F2), 15.5% of the total variance, showed a strong correlation with Ni, Co, Cr, V, Hg, Zn, Ti, and Mn. These elements, especially V and Ni at high concentrations, are usual constituents of the asphalt pavement (e.g., Dehghani et al. 2017), which is widely used in Cuban roads.

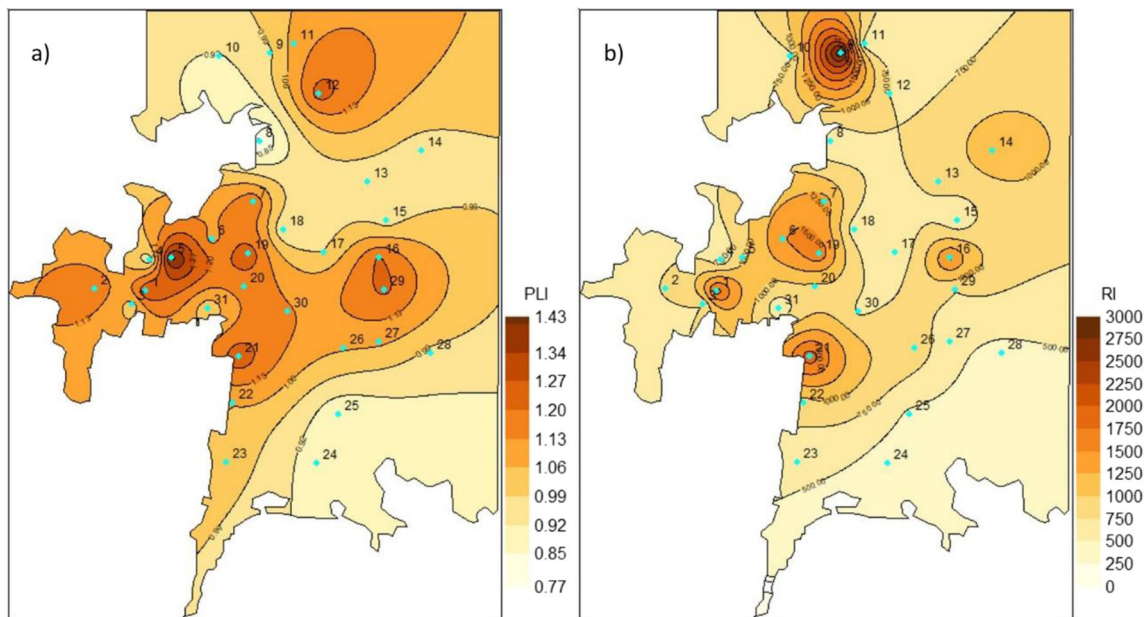


Fig. 4 Distribution patterns for (a) the pollution load index (PLI) and (b) the ecological risk index (RI) calculated from road dust samples in Cienfuegos, Cuba

Similarly, Ni, Cr, Ti, and Mn are common constituents of the pavement aggregates (rocks, sands..., Kupiainen et al. 2005; Manno et al. 2006; Li et al. 2016). Thus, factor 2 shows that road pavement wear is an important source for these elements. The associated moderate Hg factor loading (0.549) indicates that road pavement, although a potential source, is not the unique source of Hg in the dust. In addition, high concentrations of V, Ni, Ti, and Zn were measured in fly and bottom ashes emitted by the combustion of Cuban heavy crude oil from the power plant located in the city (Alonso-Hernandez et al. 2011; Morera-Gómez et al. 2018a). These emissions can also be found deposited onto urban roads.

Factor 3 (F3), 11.1% of the total variance, yielded high Pb, Sb, Cu, and Sn factor loadings, elements usually linked to road traffic (Johansson et al. 2009). These elements were moderately to highly enriched and strongly correlated in our samples. Cu, Sb, and Sn have been extensively used as specific tracers for brake wear (Sternbeck et al. 2002; e.g. Adachi and Tainosho 2004; Grigoratos and Martini 2015). Although mostly phased out worldwide since the 1990s, the combustion

of leaded gasoline is still associated with the presence of Pb in street dust as it is a persistent element showing poor mobility (Keshavarzi et al. 2018). However, road traffic in Cuba is dominated by diesel cars. Other potential sources of Pb include exterior paints, industrial emissions, and wastes (Taiwo et al. 2014; Keshavarzi et al. 2018). In factor 4 (F4), accounting for 9.5% of the total variance, S, Mo, and W were strongly associated (Table 2) and TC presented a moderate factor loading (0.404). These elements are mostly found in industrial atmospheric emissions (Taiwo et al. 2014). Here, they were moderately to highly enriched, confirming the anthropogenic origin of these elements in Cienfuegos. Combustion of the sulfur-rich Cuban crude oil by the local power plant has been connected to high S and TC contents in Cienfuegos ambient aerosols (Morera-Gómez et al. 2018a, b). High Mo concentrations have also been observed in bottom ashes from this power plant (Alonso-Hernandez et al. 2011). Mo-bearing compounds, including molybdenite (MoS_2), are used as catalyzers in oil refining and petrochemical processes (Abbasi et al. 2018), as lubricants and are present in

Table 1 Statistic summary of calculated E_r^i and RI values

| | E_r^i | | | | | | | | | | | | | | RI |
|--------------------|---------|-----|-----|-----|-----|-----|-----|-----|-----|------|-----|-----|-----|------|------|
| | V | Cr | Mn | Co | Ni | Cu | Zn | As | Sr | Cd | Pb | Ti | Sb | Hg | |
| Mean | 4 | 4 | 1 | 4 | 7 | 19 | 4 | 12 | 1 | 398 | 40 | 1 | 57 | 392 | 945 |
| Min | 2 | 2 | 1 | 3 | 4 | 8 | 2 | 6 | 1 | 233 | 15 | 1 | 22 | 69 | 391 |
| Max | 8 | 6 | 2 | 6 | 11 | 67 | 13 | 24 | 1 | 971 | 111 | 1 | 131 | 2270 | 2957 |
| SD | 1 | 1 | 0 | 1 | 2 | 11 | 2 | 5 | 0 | 145 | 24 | 0 | 25 | 499 | 569 |
| Fraction of RI (%) | 0.4 | 0.4 | 0.1 | 0.5 | 0.7 | 2.0 | 0.4 | 1.3 | 0.1 | 42.2 | 4.2 | 0.1 | 6.1 | 41.5 | |

Table 2 Factor loadings for the Varimax rotated principal components

| Element | Component | | | | |
|---------------|-----------|--------|--------|--------|--------|
| | F1 | F2 | F3 | F4 | F5 |
| K | 0.941 | -0.203 | 0.045 | 0.037 | -0.047 |
| Na | 0.897 | -0.007 | 0.154 | -0.074 | -0.051 |
| Ca | -0.779 | -0.137 | -0.162 | 0.054 | -0.256 |
| Mn | 0.762 | 0.473 | 0.174 | -0.037 | -0.032 |
| Fe | 0.755 | 0.342 | 0.300 | 0.198 | -0.055 |
| Ti | 0.735 | 0.513 | 0.214 | -0.196 | -0.071 |
| As | 0.702 | 0.162 | 0.328 | 0.190 | 0.154 |
| TC | -0.563 | -0.190 | -0.072 | 0.404 | 0.487 |
| Ni | -0.032 | 0.898 | 0.172 | 0.110 | 0.111 |
| Co | 0.342 | 0.802 | -0.083 | 0.113 | -0.037 |
| Cr | 0.022 | 0.797 | 0.086 | -0.194 | -0.245 |
| V | 0.390 | 0.607 | 0.326 | -0.164 | 0.172 |
| Hg | 0.144 | 0.549 | 0.352 | -0.095 | 0.347 |
| Zn | 0.121 | 0.524 | 0.395 | 0.180 | 0.470 |
| Pb | 0.128 | 0.040 | 0.861 | 0.125 | -0.050 |
| Sb | 0.169 | 0.197 | 0.853 | 0.070 | 0.222 |
| Cu | 0.253 | 0.178 | 0.850 | -0.026 | 0.077 |
| Sn | 0.250 | 0.113 | 0.802 | -0.073 | -0.034 |
| S | -0.065 | 0.014 | -0.002 | 0.895 | 0.019 |
| Mo | -0.005 | 0.136 | -0.127 | 0.727 | 0.452 |
| W | 0.076 | -0.146 | 0.204 | 0.723 | 0.123 |
| TN | 0.030 | 0.117 | -0.137 | 0.322 | 0.790 |
| Cd | 0.014 | -0.086 | 0.257 | 0.042 | 0.771 |
| Eigenvalues | 8.070 | 3.573 | 2.555 | 2.189 | 1.224 |
| % of variance | 35.09 | 15.54 | 11.11 | 9.52 | 5.32 |
| Cumulative % | 35.09 | 50.62 | 61.73 | 71.25 | 76.57 |

motorcycle brake pads. W, on the other hand, has been found at low concentrations in brake wear (Johansson et al. 2009). The last factor (F5) explained 5.3% of the variance and was represented by high TN and Cd factor loadings. High Cd and N levels are typical of a wide range of urban sources, including paints, solid wastes, wastewaters, and fertilizers (Li et al. 2018a; Modabberi et al. 2018). As discussed above, organic matter appears as a major source of N road dust in Cienfuegos.

Finally, sampling sites were classified into four distinct groups following a hierarchical cluster analysis based on their chemical and stable C and N isotope compositions (Fig. 5). Cluster 1 represents the contribution from the pavement wear and includes the sites with the highest Zn, Ni, Cr, Co, and Hg average concentrations. Cluster 2 yielded the highest Cu, Sb, Sn, As, and Pb average concentrations coupled to the lowest $\delta^{13}C$, identifying sites mostly affected by road traffic. These first two clusters regroup sites that are located on the busiest roads, intersections, and highways of the city, confirming the conclusions that we drew from the PCA. Cluster 3 includes the sampling sites that yielded the lowest average concentrations

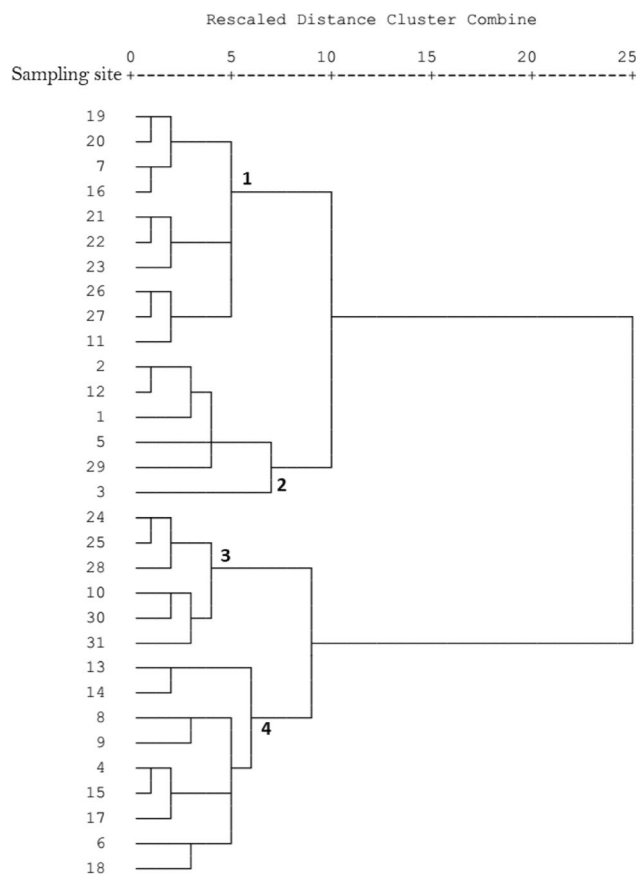


Fig. 5 Dendrogram obtained by hierarchical cluster analysis using the Ward’s method criterion

for most of the potentially toxic elements as well as the lowest $\delta^{15}N$ values. These sites are mainly located in residential areas with low road traffic. Cluster 4 corresponds to sites with the highest average Ca and TC concentrations and the highest $\delta^{13}C$ indicating a strong carbonate contribution, probably emitted by the cement production, construction, and related activities. These sites also had the highest average S, W, and Mo concentrations, which may be related to the emissions from the power plant. Several of this cluster’s sites (4, 6, 8, and 9) are the closest to the city power plant (~ 1.0–1.5 km). Moreover, cluster 4 includes the sites with the highest Cd and TN concentrations and the highest $\delta^{15}N$, probably explained by the fact that most of these sites (in particular sites 13–15, 17, and 18) are routes frequently used by horse-drawn carriages and thus are commonly impacted by organic matter inputs.

Implications for environmental and human health

Road dust is constituted by a complex mixture of particles, among which the smaller fraction may be resuspended by physical processes and thus poses a respiratory risk to human health (LeGalley et al. 2013 and reference therein). The presence of potentially toxic metals, organic compounds, and other associated contaminants may also have environmental

impacts (Abbasi et al. 2017; Modabberi et al. 2018). Ultimately, road dust and its associated contaminants can play a critical role in degrading the quality of receiving water bodies (Sutherland and Tolosa 2000). Cienfuegos Bay is subject to important road runoff either directly or through drainage systems, especially during the wet season when this study was conducted. Road runoff discharge into the Bay may also carry a significant amount of nutrients. The availability of these nutrients in excess to this coastal ecosystem is also a key factor that, coupled with the local high salinity, temperature, irradiance, and water residence time, can contribute to toxic algal blooms (Walsh et al. 2006; Cuellar-Martinez et al. 2018). Recently, such events occurred at popular beaches in Cienfuegos Bay and were linked to skin lesions, specially impacting children (Moreira González et al. 2016).

Cienfuegos local authorities now invest considerable efforts and resources to monitoring local environment, including water quality in the Cienfuegos Bay (Seisdedo et al. 2016, 2019). Our results should help them design a more effective implementation of environmental management measures against water, soil, and air contamination in Cienfuegos. Several cities worldwide have already implemented sweeping and street cleaning systems that collect dusts in dedicated containers (Manuel Trujillo-Gonzalez et al. 2016 and references therein; Lloyd et al. 2019). Proper disposal of solid waste and more efficient wastewater drainage systems are now also issues of increasing concern for local governments.

Conclusions

An exhaustive chemical and stable C and N isotope composition characterization of road dust was conducted for first time in the mid-size city of Cienfuegos in Cuba, helping us to better understand the contamination spatial distribution and the implication of the different sources that adversely impact the local environment quality.

Results show that the $\delta^{13}\text{C}$ of road dust identify the presence of carbonates that can be related to atmospheric emissions from the cement plant and related activities (construction, work in quarries, transportation of cement and raw materials...). The $\delta^{15}\text{N}$, on the other hand, shows a ^{15}N depletion with the decrease of the TN content, indicating nitrogen isotope fractionations induced by secondary processes. Comparison with the characteristics of potential sources of contamination allows us to conclude that primary nitrogen may mainly be generated by POM inputs. Both the pollution load and the ecological risk indexes demonstrate that road dust in Cienfuegos is contaminated and have associated high ecological risks, especially along busy roads and downtown. The PCA analysis identifies the major local sources of contamination: mineral matter from the soil, atmospheric emissions by the cement plant and related

activities, road pavement alteration, atmospheric emissions by the power plant, road traffic, and POM.

Our results suggest that the chemical and isotope monitoring of road dust should be included in future overall contamination management schemes.

Funding information This research has received funding from the “la Caixa” Banking Foundation. The study was also supported by the IAEA TC Project CUB/7/008 “Strengthening the National System for Analysis of the Risks and Vulnerability of Cuba’s Coastal Zone Through the Application of Nuclear and Isotopic Techniques” and National Program PNUOLU /4-1/ 2 No. /2014 of the National Nuclear Agency.

References

- Abbasi S, Keshavarzi B, Moore F, Delshab H, Soltani N, Sorooshian A (2017) Investigation of microrubbers, microplastics and heavy metals in street dust: a study in Bushehr city, Iran. *Environ Earth Sci* 76:798–719. <https://doi.org/10.1007/s12665-017-7137-0>
- Abbasi S, Keshavarzi B, Moore F, Mahmoudi MR (2018) Fractionation, source identification and risk assessment of potentially toxic elements in street dust of the most important center for petrochemical products, Asaluyeh County, Iran. *Environ Earth Sci* 77:673–619. <https://doi.org/10.1007/s12665-018-7854-z>
- Adachi K, Tainosho Y (2004) Characterization of heavy metal particles embedded in tire dust. *Environment International* 30:1009–1017. <https://doi.org/10.1016/j.envint.2004.04.004>
- Adamiec E, Jarosz-Krzemińska E, Wieszała R (2016) Heavy metals from non-exhaust vehicle emissions in urban and motorway road dusts. *Environmental Monitoring and Assessment* 188:369. <https://doi.org/10.1007/s10661-016-5377-1>
- Alfaro MR, Montero A, Ugarte OM, do Nascimento CW, de Aguiar Accioly AM, Biondi CM, da Silva YJ (2015) Background concentrations and reference values for heavy metals in soils of Cuba. *Environ Monit Assess* 187:4198. <https://doi.org/10.1007/s10661-014-4198-3>
- Alfaro MR, do Nascimento CWA, Biondi CM et al (2018) Rare-earth-element geochemistry in soils developed in different geological settings of Cuba. *CATENA* 162:317–324. <https://doi.org/10.1016/j.catena.2017.10.031>
- Alonso-Hernandez CM, Bernal-Castillo J, Bolanos-Alvarez Y et al (2011) Heavy metal content of bottom ashes from a fuel oil power plant and oil refinery in Cuba. *Fuel* 90:2820–2823. <https://doi.org/10.1016/j.fuel.2011.03.014>
- Alonso-Hernández CM, Garcia-Moya A, Tolosa I et al (2017) Tracing organic matter sources in a tropical lagoon of the Caribbean Sea. *Cont Shelf Res* 148:53–63. <https://doi.org/10.1016/j.csr.2017.08.001>
- Alves CA, Evtuygina M, Vicente AMP, Vicente ED, Nunes TV, Silva PMA, Duarte MAC, Pio CA, Amato F, Querol X (2018) Chemical profiling of PM 10 from urban road dust. *Sci Total Environ* 634:41–51. <https://doi.org/10.1016/j.scitotenv.2018.03.338>
- Amiri H, Zare M, Widory D (2015) Assessing sources of nitrate contamination in the Shiraz urban aquifer (Iran) using the $\delta^{15}\text{N}$ and $\delta^{18}\text{O}$ dual-isotope approach. *Isotopes Environ Health Stud* 51:392–410. <https://doi.org/10.1080/10256016.2015.1032960>
- Andrews JE, Greenaway AM, Dennis PF (1998) Combined carbon isotope and C/N ratios as indicators of source and fate of organic matter in a poorly flushed, tropical estuary: Hunts Bay, Kingston Harbour, Jamaica. *Estuar Coast Shelf Sci* 46:743–756. <https://doi.org/10.1006/ecss.1997.0305>
- Asar Ö, İlk Ö, Dag O (2017) Estimating Box-Cox power transformation parameter via goodness-of-fit tests. *Commun Stat Simul Comput* 46:91–105. <https://doi.org/10.1080/03610918.2014.957839>

- Bandowe BAM, Nkansah MA, Leimer S, Fischer D, Lammel G, Han Y (2018) Chemical (C, N, S, black carbon, soot and char) and stable carbon isotope composition of street dusts from a major West African metropolis: implications for source apportionment and exposure. *Sci Total Environ* 655:1468–1478. <https://doi.org/10.1016/j.scitotenv.2018.11.089>
- Bourliva A, Christophoridis C, Papadopoulou L, Giouri K, Papadopoulos A, Mitsika E, Fytianos K (2017) Characterization, heavy metal content and health risk assessment of urban road dusts from the historic center of the city of Thessaloniki, Greece. *Environ Geochem Health* 39:611–634. <https://doi.org/10.1007/s10653-016-9836-y>
- Bourliva A, Kantiranis N, Papadopoulou L et al (2018) Seasonal and spatial variations of magnetic susceptibility and potentially toxic elements (PTEs) in road dusts of Thessaloniki city, Greece: a one-year monitoring period. *Sci Total Environ* 639:417–427. <https://doi.org/10.1016/j.scitotenv.2018.05.170>
- Celo V, Dabek-Zlotorzynska E, Zhao J, Bowman D (2012) Concentration and source origin of lanthanoids in the Canadian atmospheric particulate matter: a case study. *Atmos Pollut Res* 3:270–278. <https://doi.org/10.5094/APR.2012.030>
- Christoforidis A, Stamatis N (2009) Heavy metal contamination in street dust and roadside soil along the major national road in Kavala's region, Greece. *Geoderma* 151:257–263. <https://doi.org/10.1016/j.geoderma.2009.04.016>
- Cuellar-Martinez T, Ruiz-Fernández AC, Alonso-Hernández C et al (2018) Addressing the problem of harmful algal blooms in Latin America and the Caribbean- a regional network for early warning and response. *Front Mar Sci* 5. <https://doi.org/10.3389/fmars.2018.00409>
- Das A, Krishna KVSS, Kumar R, Saha MC, Sengupta S, Ghosh JG (2017) Lead isotopic ratios in source apportionment of heavy metals in the street dust of Kolkata, India. *Int J Environ Sci Technol* 15:1–14. <https://doi.org/10.1007/s13762-017-1377-0>
- Dehghani S, Moore F, Keshavarzi B, Hale BA (2017) Health risk implications of potentially toxic metals in street dust and surface soil of Tehran, Iran. *Ecotox Environ Safe* 136:92–103. <https://doi.org/10.1016/j.ecoenv.2016.10.037>
- Díaz Rizo O, Rivero Plama O, D'Alessandro Rodríguez K, García Trápaga C (2015) Distribución espacial y estudio de contaminación por metales pesados en polvos urbanos de la ciudad de Camagüey (Cuba) mediante fluorescencia de rayos X. *Nucleus* 58:34–38
- Fattorini D, Alonso-Hernandez CM, Diaz-Asencio M, Munoz-Caravaca A, Pannacciulli FG, Tangherlini M, Regoli F (2004) Chemical speciation of arsenic in different marine organisms: importance in monitoring studies. *Marine Environmental Research* 58:845–850. <https://doi.org/10.1016/j.marenvres.2004.03.103>
- Ferreira-Baptista L, De Miguel E (2005) Geochemistry and risk assessment of street dust in Luanda, Angola: a tropical urban environment. *Atmos Environ* 39:4501–4512. <https://doi.org/10.1016/j.atmosenv.2005.03.026>
- Ghanavati N, Nazarpour A, Watts MJ (2019) Status, source, ecological and health risk assessment of toxic metals and polycyclic aromatic hydrocarbons (PAHs) in street dust of Abadan, Iran. *CATENA* 177: 246–259. <https://doi.org/10.1016/j.catena.2019.02.022>
- Grigoratos T, Martini G (2015) Brake wear particle emissions: a review. *Environmental Science and Pollution Research* 22:2491–2504. <https://doi.org/10.1007/s11356-014-3696-8>
- Hakanson L (1980) An ecological risk index for aquatic pollution control. A sedimentological approach. *Water Res* 14:975–1001. [https://doi.org/10.1016/0043-1354\(80\)90143-8](https://doi.org/10.1016/0043-1354(80)90143-8)
- Johansson C, Norman M, Burman L (2009) Road traffic emission factors for heavy metals. *Atmos Environ* 43:4681–4688. <https://doi.org/10.1016/j.atmosenv.2008.10.024>
- Kawashima H, Haneishi Y (2012) Effects of combustion emissions from the Eurasian continent in winter on seasonal $\delta^{13}C$ of elemental carbon in aerosols in Japan. *Atmos Environ* 46:568–579. <https://doi.org/10.1016/j.atmosenv.2011.05.015>
- Keshavarzi B, Abbasi S, Moore F, Mehravar S, Sorooshian A, Soltani N, Najmeddin A (2018) Contamination level, source identification and risk assessment of potentially toxic elements (PTEs) and polycyclic aromatic hydrocarbons (PAHs) in street dust of an important commercial center in Iran. *Environ Manage* 62:803–818. <https://doi.org/10.1007/s00267-018-1079-5>
- Kojima K, Murakami M, Yoshimizu C, Tayasu I, Nagata T, Furumai H (2011) Evaluation of surface runoff and road dust as sources of nitrogen using nitrate isotopic composition. *Chemosphere* 84: 1716–1722. <https://doi.org/10.1016/j.chemosphere.2011.04.071>
- Kojima K, Sano S, Kurisu F, Furumai H (2017) Estimation of source contribution to nitrate loading in road runoff using stable isotope analysis. *Urban Water J* 14:337–342. <https://doi.org/10.1080/1573062X.2016.1148176>
- Kump LR, Arthur MA (1999) Interpreting carbon-isotope excursions: carbonates and organic matter. *Chem Geol* 161:181–198. [https://doi.org/10.1016/S0009-2541\(99\)00086-8](https://doi.org/10.1016/S0009-2541(99)00086-8)
- Kupiainen KJ, Tervahattu H, Räisänen M, Mäkelä T, Aurela M, Hillamo R (2005) Size and composition of airborne particles from pavement wear, tires, and traction sanding. *Environ Sci Technol* 39:699–706. <https://doi.org/10.1021/es035419e>
- Lanzerstorfer C (2018) Heavy metals in the finest size fractions of road-deposited sediments. *Environ Pollut* 239:522–531. <https://doi.org/10.1016/j.envpol.2018.04.063>
- LeGalley E, Widom E, Krekeler MPS, Kuentz DC (2013) Chemical and lead isotope constraints on sources of metal pollution in street sediment and lichens in southwest Ohio. *Appl Geochem* 32:195–203. <https://doi.org/10.1016/j.apgeochem.2012.10.020>
- Li Z, Feng X, Li G et al (2013) Distributions, sources and pollution status of 17 trace metal/metalloids in the street dust of a heavily industrialized city of central China. *Environ Pollut* 182:408–416. <https://doi.org/10.1016/j.envpol.2013.07.041>
- Li Y, Yu Y, Yang Z, Shen Z, Wang X, Cai Y (2016) A comparison of metal distribution in surface dust and soil among super city, town, and rural area. *Environ Sci Pollut Res* 23:7849–7860. <https://doi.org/10.1007/s11356-015-5911-7>
- Li F, Jinxu Y, Shao L et al (2018a) Delineating the origin of Pb and Cd in the urban dust through elemental and stable isotopic ratio: a study from Hangzhou City, China. *Chemosphere* 211:674–683. <https://doi.org/10.1016/j.chemosphere.2018.07.199>
- Li X, Zhang M, Gao Y et al (2018b) Urban street dust bound 24 potentially toxic metal/metalloids (PTMs) from Xining valley-city, NW China: spatial occurrences, sources and health risks. *Ecotox Environ Safe* 162:474–487. <https://doi.org/10.1016/j.ecoenv.2018.07.006>
- Li X, Liu B, Zhang Y et al (2019) Spatial distributions, sources, potential risks of multi-trace metal/metalloids in street dusts from Barbican Downtown embracing by Xi'an Ancient City Wall (NW, China). *Int J Environ Res Public Health* 16:2992. <https://doi.org/10.3390/ijerph16162992>
- Lloyd LN, Fitch GM, Singh TS, Smith JA (2019) Characterization of environmental pollutants in sediment collected during street sweeping operations to evaluate its potential for reuse. *J Environ Eng-ASCE* 145:04018141. [https://doi.org/10.1061/\(ASCE\)EE.1943-7870.0001493](https://doi.org/10.1061/(ASCE)EE.1943-7870.0001493)
- Lopez-Veneroni D (2009) The stable carbon isotope composition of PM_{2.5} and PM₁₀ in Mexico City Metropolitan Area air. *Atmos Environ* 43:4491–4502. <https://doi.org/10.1016/j.atmosenv.2009.06.036>
- Manno E, Varrica D, Dongarra G (2006) Metal distribution in road dust samples collected in an urban area close to a petrochemical plant at Gela, Sicily. *Atmos Environ* 40:5929–5941. <https://doi.org/10.1016/j.atmosenv.2006.05.020>
- Manuel Trujillo-Gonzalez J, Aurelio Torres-Mora M, Keesstra S et al (2016) Heavy metal accumulation related to population density in

- road dust samples taken from urban sites under different land uses. *Sci Total Environ* 553:636–642. <https://doi.org/10.1016/j.scitotenv.2016.02.101>
- Mari M, Sanchez-Soberon F, Audi-Miro C et al (2016) Source apportionment of inorganic and organic PM in the ambient air around a cement plant: assessment of complementary tools. *Aerosol Air Qual Res* 16:3230–3242. <https://doi.org/10.4209/aaqr.2016.06.0276>
- Men C, Liu R, Wang Q, Guo L, Shen Z (2018) The impact of seasonal varied human activity on characteristics and sources of heavy metals in metropolitan road dusts. *Sci Total Environ* 637:844–854. <https://doi.org/10.1016/j.scitotenv.2018.05.059>
- Modabberri S, Tashakor M, Soltani NS, Hursthouse AS (2018) Potentially toxic elements in urban soils: source apportionment and contamination assessment. *Environ Monit Assess* 190:715–718. <https://doi.org/10.1007/s10661-018-7066-8>
- Moreira González A, Abilio Comas A, Valle Pombrol A, Seisdedo M (2016) Bloom of *Vulcanodinium rugosum* linked to skin lesions in Cienfuegos Bay, Cuba. *HARMFUL ALGAE NEWS* 55
- Moreno T, Querol X, Alastuey A, Gibbons W (2008) Identification of FCC refinery atmospheric pollution events using lanthanoid- and vanadium-bearing aerosols. *Atmos Environ* 42:7851–7861. <https://doi.org/10.1016/j.atmosenv.2008.07.013>
- Moreno T, Querol X, Alastuey A et al (2010) Variations in vanadium, nickel and lanthanoid element concentrations in urban air. *Sci Total Environ* 408:4569–4579. <https://doi.org/10.1016/j.scitotenv.2010.06.016>
- Morera-Gómez Y, Elustondo D, Lasheras E et al (2018a) Chemical characterization of PM10 samples collected simultaneously at a rural and an urban site in the Caribbean coast: local and long-range source apportionment. *Atmos Environ* 192:182–192. <https://doi.org/10.1016/j.atmosenv.2018.08.058>
- Morera-Gómez Y, Santamaría JM, Elustondo D, Alonso-Hernández CM, Widory D (2018b) Carbon and nitrogen isotopes unravels sources of aerosol contamination at Caribbean rural and urban coastal sites. *Sci Total Environ* 642:723–732. <https://doi.org/10.1016/j.scitotenv.2018.06.106>
- Morera-Gómez Y, Santamaría JM, Elustondo D et al (2019) Determination and source apportionment of major and trace elements in atmospheric bulk deposition in a Caribbean rural area. *Atmos Environment* 202:93–104. <https://doi.org/10.1016/j.atmosenv.2019.01.019>
- Pateraki St, Manousakas M, Bairachtari K et al (2019) The traffic signature on the vertical PM profile: environmental and health risks within an urban roadside environment. *Sci Total Environ* 646:448–459. <https://doi.org/10.1016/j.scitotenv.2018.07.28>
- Rasmussen PE, Subramanian KS, Jessiman BJ (2001) A multi-element profile of house dust in relation to exterior dust and soils in the city of Ottawa, Canada. *Sci Total Environ* 267:125–140. [https://doi.org/10.1016/S0048-9697\(00\)00775-0](https://doi.org/10.1016/S0048-9697(00)00775-0)
- Rudnick RL, Gao S (2014) Composition of the continental crust. In: Holland HD, Turekian KK (eds) *Treatise on Geochemistry*, Second edn. Elsevier, Oxford, pp 1–51
- Seisdedo M, Herrera RH, Arencibia G, Sorinas L (2016) Tools for managing water quality from trophic state in the estuarine system Cienfuegos bay (Cuba). *Pan-Am J Aquat Sci* 11:264–275
- Seisdedo M, Castellanos González ME, Arencibia Carballo G et al (2019) Water quality management in Cienfuegos Bay (Cuba) with integrative approaches. *Int J Environ Agric Biotechnol* 4:182–186. <https://doi.org/10.22161/ijeab/4.1.28>
- Shi D, Lu X (2018) Accumulation degree and source apportionment of trace metals in smaller than 63 μm road dust from the areas with different land uses: a case study of Xi'an, China. *Sci Total Environ* 636:1211–1218. <https://doi.org/10.1016/j.scitotenv.2018.04.385>
- Skrbic BD, Buljovicic M, Jovanovic G, Antic I (2018) Seasonal, spatial variations and risk assessment of heavy elements in street dust from Novi Sad, Serbia. *Chemosphere* 205:452–462. <https://doi.org/10.1016/j.chemosphere.2018.04.124>
- Škrbić B, Đurišić-Mladenović N, Živančević J, Tadić Đ (2019) Seasonal occurrence and cancer risk assessment of polycyclic aromatic hydrocarbons in street dust from the Novi Sad city, Serbia. *Sci Total Environ* 647:191–203. <https://doi.org/10.1016/j.scitotenv.2018.07.442>
- Soltani N, Keshavarzi B, Moore F, Tavakol T, Lahijanzadeh AR, Jaafarzadeh N, Kermani M (2015) Ecological and human health hazards of heavy metals and polycyclic aromatic hydrocarbons (PAHs) in road dust of Isfahan metropolis, Iran. *Sci Total Environ* 505:712–723. <https://doi.org/10.1016/j.scitotenv.2014.09.097>
- Soonthornnonda P, Christensen ER (2008) Source apportionment of pollutants and flows of combined sewer wastewater. *Water Res* 42:1989–1998. <https://doi.org/10.1016/j.watres.2007.11.034>
- Sternbeck J, Sjödin Å, Andréasson K (2002) Metal emissions from road traffic and the influence of resuspension—results from two tunnel studies. *Atmos Environ* 36:4735–4744. [https://doi.org/10.1016/S1352-2310\(02\)00561-7](https://doi.org/10.1016/S1352-2310(02)00561-7)
- Sutherland RA, Tolosa CA (2000) Multi-element analysis of road-deposited sediment in an urban drainage basin, Honolulu, Hawaii. *Environ Pollut* 110:483–495. [https://doi.org/10.1016/S0269-7491\(99\)00311-5](https://doi.org/10.1016/S0269-7491(99)00311-5)
- Taiwo AM, Harrison RM, Shi Z (2014) A review of receptor modelling of industrially emitted particulate matter. *Atmos Environ* 97:109–120. <https://doi.org/10.1016/j.atmosenv.2014.07.051>
- Tomlinson DL, Wilson JG, Harris CR, Jeffrey DW (1980) Problems in the assessment of heavy-metal levels in estuaries and the formation of a pollution index. *Helgolander Meeresunters* 33:566–575. <https://doi.org/10.1007/BF02414780>
- Walsh JJ, Jolliff JK, Darrow BP, Lenos JM, Milroy SP, Remsen A, Dieterle DA, Carder KL, Chen FR, Vargo GA, Weisberg RH, Fanning KA, Muller-Karger FE, Shinn E, Steidinger KA, Heil CA, Tomas CR, Prospero JS, Lee TN, Kirkpatrick GJ, Whitledge TE, Stockwell DA, Villareal TA, Jochens AE, Bontempi PS (2006) Red tides in the Gulf of Mexico: Where, when, and why? *J Geophys Res* 111:1–46. <https://doi.org/10.1029/2004JC002813>
- Wei B, Jiang F, Li X, Mu S (2009) Spatial distribution and contamination assessment of heavy metals in urban road dusts from Urumqi, NW China. *Microchem J* 93:147–152. <https://doi.org/10.1016/j.micro.2009.06.001>
- WHO (2016) WHO | WHO releases country estimates on air pollution exposure and health impact. In: WHO. <http://www.who.int/mediacentre/news/releases/2016/air-pollution-estimates/en/>. Accessed 21 Mar 2017
- Xu D-M, Zhang J-Q, Yan B, Liu H, Zhang LL, Zhan CL, Zhang L, Zhong P (2018) Contamination characteristics and potential environmental implications of heavy metals in road dusts in typical industrial and agricultural cities, southeastern Hubei Province, Central China. *Environ Sci Pollut Res* 25:36223–36238. <https://doi.org/10.1007/s11356-018-3282-6>
- Yu Y, Li Y, Li B, Shen Z, Stenstrom MK (2016) Metal enrichment and lead isotope analysis for source apportionment in the urban dust and rural surface soil. *Environ Pollut* 216:764–772. <https://doi.org/10.1016/j.envpol.2016.06.046>
- Zhang J, Li R, Zhang X, Bai Y, Cao P, Hua P (2019) Vehicular contribution of PAHs in size dependent road dust: A source apportionment by PCA-MLR, PMF, and Unmix receptor models. *Sci Total Environ* 649:1314–1322. <https://doi.org/10.1016/j.scitotenv.2018.08.410>

Publisher's note Springer Nature remains neutral with regard to jurisdictional claims in published maps and institutional affiliations.

Reproduced with permission of copyright owner. Further reproduction prohibited without permission.